Published in final edited form as:
Anesth Analg. 2013 April ; 116(4): 869–880. doi:10.1213/ANE.0b013e3182860fc9.

Ketamine Enhances Human Neural Stem Cell Proliferation and Induces Neuronal Apoptosis Via Reactive Oxygen Species-Mediated Mitochondrial Pathway

Xiaowen Bai, MD, PhD
Department of Anesthesiology, Medical College of Wisconsin, Milwaukee, Wisconsin

Yasheng Yan, BS
Department of Anesthesiology, Medical College of Wisconsin, Milwaukee, Wisconsin

Scott Canfield, BS
Department of Anesthesiology and Physiology, Medical College of Wisconsin, Milwaukee, Wisconsin

Maria Y. Muravyeva, MD, PhD
Department of Anesthesiology, Medical College of Wisconsin, Milwaukee, Wisconsin

Chika Kikuchi, MD

Corresponding Author: Xiaowen Bai, MD, PhD Department of Anesthesiology Medical College of Wisconsin 8701 Watertown Plank Road, Milwaukee, WI 53226 Phone: 414-456-5755 Fax: 414-456-6122 xibai@mcw.edu.

The authors declare no conflicts of interest.

DISCLOSURES: Name: Xiaowen Bai, MD, PhD
Contribution: This author helped conceptualize the study, design the study, acquire data and images, analyze and interpret the data, and write the manuscript.
Attestation: Xiaowen Bai attests to having approved the final manuscript, approved the final manuscript. Xiaowen Bai attests to the integrity of the original data and the analysis reported in this manuscript. Xiaowen Bai is the archival author
Name: Yasheng Yan, BS
Contribution: This author helped perform the experiments, acquire the data, and analyze and interpret the data.
Attestation: Yasheng Yan attests to having approved the final manuscript. Yasheng Yan attests to the integrity of the original data and the analysis reported in this manuscript
Name: Scott Canfield, BS
Contribution: This author helped perform the experiments, and analyze and interpret the data.
Attestation: Scott Canfield attests to having approved the final manuscript
Name: Maria Y. Muravyeva, MD, PhD
Contribution: This author helped analyze the data.
Attestation: Maria Y. Muravyeva attests to having approved the final manuscript
Name: Chika Kikuchi, MD
Contribution: This author helped perform the experiments, and analyze and interpret the data.
Attestation: Chika Kikuchi attests to having approved the final manuscript
Name: Ivan Zaja, MD
Contribution: This author helped perform the experiments, acquire the data, and analyze and interpret the data.
Attestation: Ivan Zaja attests to having approved the final manuscript
Name: John A. Corbett, PhD
Contribution: This author helped analyze and interpret the data.
Attestation: John A. Corbett attests to having approved the final manuscript
Name: Zeljko J. Bosnjak, PhD
Contribution: This author helped conceptualize the study, design the study, and analyze and interpret the data, and write the manuscript.
Attestation: Zeljko J. Bosnjak attests to having approved the final manuscript

Department of Anesthesiology, Medical College of Wisconsin, Milwaukee, Wisconsin

Ivan Zaja, MD
Department of Anesthesiology, Medical College of Wisconsin, Milwaukee, Wisconsin

John A. Corbett, PhD
Department of Biochemistry, Medical College of Wisconsin, Milwaukee, Wisconsin

Zeljko J. Bosnjak, PhD
Departments of Anesthesiology and Physiology, Medical College of Wisconsin, Milwaukee, Wisconsin

Abstract

Background—Growing evidence indicates that ketamine causes neurotoxicity in a variety of developing animal models, leading to a serious concern regarding the safety of pediatric anesthesia. However, if and how ketamine induces human neural cell toxicity is unknown. Recapitulation of neurogenesis from human embryonic stem cells (hESCs) *in vitro* allows investigation of the toxic effects of ketamine on neural stem cells (NSCs) and developing neurons which is impossible to perform in humans. In the present study we assessed the influence of ketamine on the hESC-derived NSCs and neurons.

Methods—hESCs were directly differentiated into neurons via NSCs. NSCs and two-week-old neurons were treated with varying doses of ketamine for different durations. NSC proliferation capacity was analyzed by Ki67 immunofluorescence staining and bromodeoxyurindine assay. Neuroapoptosis was analyzed by TUNEL staining and caspase 3 activity measurement. The mitochondria-related neuronal apoptosis pathway including mitochondrial membrane potential, cytochrome c distribution within cells, mitochondrial fission, and reactive oxygen species (ROS) production were also investigated.

Results—Ketamine (100 μM) increased NSC proliferation after 6 h exposure. However, significant neuronal apoptosis was only observed after 24 h of ketamine treatment. In addition, ketamine decreased mitochondrial membrane potential and increased cytochrome c release from mitochondria into cytosol. Ketamine also enhanced mitochondrial fission as well as ROS production compared with no-treatment control. Importantly, Trolox, a ROS scavenger, significantly attenuated the increase of ketamine-induced ROS production and neuronal apoptosis.

Conclusions—These data for the first time demonstrate that (1) ketamine increases NSC proliferation and causes neuronal apoptosis; (2) mitochondria are involved in ketamine-induced neuronal toxicity which can be prevented by Trolox; and (3) the stem cell-associated neurogenesis system may provide a simple and promising *in vitro* model for rapidly screening anesthetic neurotoxicity and studying the underlying mechanisms as well as prevention strategies to avoid this toxic effect.

Introduction

Growing evidence suggests that prolonged exposure of developing animals during brain growth spurt to general anesthetics induces widespread neuronal cell death followed by long-term memory and learning abnormalities.[1–4] Ketamine is widely used in pediatric anesthesia to provide sedation/analgesia to children for painful procedures.[5] In addition, ketamine is one of the most studied anesthetics for addressing neurotoxicity issues in both rodent and primate models. For instance, ketamine administered subcutaneously to 7-day-old mice for 5 h resulted in a significant increase in neuronal cell death.[6] Intravenous administration of ketamine for 24 h caused an increase of cell death in the cortex of rhesus monkeys at 122 days of gestation and postnatal day 5.[4] *In vitro* experimental evidence from cultured neonatal animal neurons confirmed the *in vivo* findings.[7–14] Apoptosis was

involved in anesthetic-induced neuronal cell death.[15–18] However, the mechanistic details by which anesthetics induce neurotoxicity have yet to be established.

So far, there is no direct evidence showing any such toxic effect in human neonates and infants at any dose of anesthetics. Every year millions of children are exposed to a variety of anesthetics. The findings from animal-related studies lead to a serious concern regarding the safety of pediatric anesthesia and raise a real question whether similar neuroapoptosis also occurs in the developing human brain. However, it is almost impossible to obtain neonatal human neurons to study anesthetic neurotoxicity. In addition, many developmental events, including neural stem cell (NSC) proliferation, neurogenesis, and synaptogenesis, occur during the brain growth spurt. Therefore, neuroapoptosis may not be the only variable to be considered in evaluating potential adverse effects of anesthetics on neuronal development. Thus, it is imperative to find a good model to study anesthetic-induced developmental neurotoxicity in human neuronal cells.

Human embryonic stem cells (hESCs) are pluripotent stem cells and can replicate indefinitely and differentiate into various cell types. Differentiation ability of hESCs into committed cell types is potentially valuable for studying cellular and molecular events involved in early human development under physiological and pathological conditions which is almost impossible to perform in humans.[19–22] In the present study, we used hESCs to recapitulate neurogenesis *in vitro* following the principles of neural development and obtained human NSCs and neurons by culturing hESCs in chemically defined medium. Using this *in vitro* hESC-related neurogenesis model, we then studied the ketamine-induced toxicity in NSCs and neurons. We hypothesized that ketamine interfered with the proliferation of hESC-derived NSCs and induced apoptosis in the human neurons differentiated from NSCs via reactive oxygen species (ROS) and mitochondrial pathway.

Methods

hESC Culture

Mitotically inactivated mouse embryonic fibroblasts (MEFs) by mitomycin C (Sigma) were used as feeder cells to support the growth and maintenance of hESCs (H1 cell line, WiCell Research Institute Inc.). Inactivated MEFs were plated in 0.1% gelatin-coated 60 mm culture Petri dishes containing Dulbecco's modified Eagle's medium (DMEM) supplemented with 10% fetal bovine serum (Gibco) in a humidified incubator under normoxic condition (20% O_2 /5% CO_2) at 37°C. On the following day, hESCs were plated on MEFs with hESC culture medium and incubated in a hypoxic incubator (4% O_2/5% CO_2). hESC culture medium consisted of DMEM/F12 supplemented with 20% KnockoutTM serum replacement (Gibco), 1% non-essential amino acids, 1% penicillin-streptomycin, 1 mM L-glutamine (Chemicon), 0.1 mM ß-mercaptoethanol (Sigma), and 4 ng/mL human recombinant basic fibroblast growth factor (bFGF; Invitrogen). The medium was changed daily. hESCs were passaged every 5–7 days using a mechanical microdissection method. hESCs with passage numbers between 70 and 80 were used in this study.

Differentiation of hESCs into Neurons

hESCs underwent four-step progression that includes embryonic body (EB) culture, rosette cell formation, NSC expansion, and neuronal differentiation as illustrated in Figure 1A and described as follows: (1) EB culture. hESCs in the culture were digested using dispase (1.5 unit/mL) (Invitrogen) for 30 min. Digested hESCs were then transferred to 60 mm ultra-low-attachment dishes (Corning) and cultured in hESC medium without bFGF under normoxic conditions. The medium was changed every day. EBs were visible one day after culturing. Four days later, EBs were switched to neural induction medium consisting of

DMEM/F12 supplemented with 1% N2 (Invitrogen), 1% non-essential amino acids, 5 ng/mL bFGF, and 1mg/mL heparin (Sigma) for 4 days. (2) Rosette formation. EBs were transferred to matrigel-coated 60 mm culture dishes and cultured with neural induction medium at day 8. The medium was changed every other day. EBs attached on the dishes and formed neural tube-like rosettes with radial arrangements of columnar cells within 5 days. (3) NSC expansion. Two days after rosette formation, rosette cells were gently blown off with a 5 ml serological and then transferred to other dishes containing DMEM/F12 supplemented with 1% N2, 2% B27 (Invitrogen), 1% non-essential amino acids, 20 ng/mL bFGF, and 1mg/mL heparin. One day later, rosette cells rolled up to form round spheres called NSCs. Half of the medium was changed every other day. NSCs were passaged every 5–6 days by digestion with accutase (Innovative Cell Technology). (4) Neuronal differentiation. Half a million NSCs were cultured in 60 mm matrigel-coated dishes with neuronal differentiation medium consisting of Neurobasal, 2% B27 (Invitrogen), 0.1 μM cyclic adenosine monophosphate, 100 ng/mL ascorbic acid (Sigma), 10 ng/mL brain-derived neurotrophic factor, 10 ng/mL glial cell-derived neurotrophic factor, and 10 ng/mL insulin-like growth factor 1 (Pepro Tech Inc.). The medium was changed every other day. Two-week-old neurons differentiated from NSCs (passages 6 to 12) were used in this study.

Ketamine Treatment

NSCs were cultured in either 60 mm dishes (with or without 12 mm coverslips) (5×10^5 cells/dish) or 96-well tissue culture plates (1×10^4 cells/well) with neuronal differentiation medium. NSCs or 2-week old differentiated neurons were incubated with or without ketamine (range 0 to 100 μM) (Phoenix Pharmaceutical Inc.) and ROS scavenger Trolox for 3, 6, or 24 h. Cell proliferation, cell viability, apoptosis, mitochondrial membrane potential ($\Delta\Psi_m$), distribution of cytochrome c in cells, mitochondrial fission, or ROS measurement were performed immediately after ketamine exposure for indicated durations. Although it was reported that peak blood levels of ketamine could be as high as 103 μM,[23] the levels required to maintain anesthesia are usually in the range of 10–20 μM.[24] Experimental evidence provided from *in vitro* cell culture and *in vivo* animal studies demonstrated that ketamine could induce neurotoxicity when administered at high doses and/or for prolonged periods.[25–29] Thus, in this study, we treated neurons with ketamine (100 μM) to study the effect of ketamine on the NSC proliferation and neuronal apoptosis for 3, 6, and 24 h. The underlying mechanisms of this side effect were investigated by exposing neurons to ketamine for 24 h.

Immunofluorescence Staining

Cells cultured on matrigel-coated coverslips were fixed with 1% paraformaldehyde for 30 min. Cells were then washed three times with phosphate buffered saline (PBS) alone or PBS containing 0.5% Triton X-100 (Sigma) and blocked with 10% donkey serum for 30 min at room temperature. Next, cells were incubated with primary antibodies in a moist chamber for 1 h at 37°C. The primary antibodies were mouse anti-stage-specific embryonic antigen 4 (SSEA-4), microtubule-associated protein 2 (MAP2), β-tubulin III (abcam), cytochrome c (BD Pharmingen), Homer 1 (Synaptic Systems), and rabbit anti-Oct-4, nestin, Ki67, synapsin-1, and PAX6. After three wash cycles, cells were incubated with Alexa Fluor 485 (or 594) donkey anti-mouse (or rabbit) immunoglobulin (IgG) (Invitrogen) for 1 h at room temperature. Cell nuclei were stained with TO-PRO®-3 (Invitrogen). The coverslips were then mounted onto the slides and observed under a laser-scanning confocal microscope (Nikon Eclipse TE2000-U). Neuronal differentiation efficiency was determined by calculating the percentage of MAP2-positive cells over the total cells. Results were obtained from at least 100 cells in each of three independently differentiated neuron samples.

Cell Proliferation Assay

The influence of ketamine on NSC proliferation was analyzed by two methods: Ki67 staining and bromodeoxyurindine (BrdU) assay. (1) Ki67 is a nuclear non-histone protein and preferentially expressed during late G1, S, G2, and M phase of the cell cycle; while resting, noncycling cells (G0 phase) lack Ki67 expression. NSCs (4×10^4 per 12 mm coverslip) were cultured in NSC medium with or without 100 μM ketamine for 3 and 6 h. Ki67 expression in NSCs was visualized using immunofluorescence staining. Ki67-positive stem cells were counted from 6 random fields per coverslip in each of three independently differentiated NSC samples. (2) BrdU incorporation as an indicator of cell proliferation was studied using a colorimetric BrdU kit (Roche Diagnostics) according to the manufacturer's instructions. BrdU is a thymidine analog and can be incorporated into newly synthesized DNA strands of actively proliferating cells. The incorporation of BrdU into cellular DNA is then detected using anti-BrdU antibody, allowing assessment of cell proliferation rate. NSCs (1×10^4 per well) were grown in 96-well plates containing NSC medium with or without 100 μM ketamine with all media being supplemented with 10 μM BrdU for either 3 or 6 h. Cells were then fixed with FixDenat solution for 30 min at room temperature followed by incubation with anti-BrdU antibody conjugated with peroxidase for 30 min. Cells were washed 3 times for 5 min each and 100 μl substrate solution was then added to the wells. Fifteen minutes later, the absorbance at 450 nm (representing proliferating potential) was measured using a microplate reader.

Analysis of Cell Ultrastructure via Electron Microscopy

Neurons cultured on matrigel-coated coverslips from each experimental condition were fixed with 2% glutaraldehyde in 0.1M sodium cacodylate buffer at 4°C, washed in the same buffer, and post-fixed with 1% osmium tetroxide for 60 min on ice. Cells were then washed briefly in distilled water and dehydrated through graded methanol (50%, 20 min; 70%, 20 min; 95%, 20 min; 100%, 3 × 20 min) and acetonitrile (2×10 min). The cells were infiltrated with epoxy resin (EMbed-812; Electron Microscopy Sciences, Hatfield, PA), and polymerized overnight at 70°C. Ultra-thin sections (~60 nm) were cut, stained with uranyl acetate and lead citrate according to standard procedures and viewed with a Hitachi H600 EM.

Caspase 3 Activity Quantification

Caspase 3 activity was measured using Caspase 3 Colorimetric Assay kit (Genescript) following the manufacturer's protocol. Neurons cultured in 60 mm dishes were washed twice with PBS and lysed with 50 μL lysis buffer followed by adding 50 μL reaction buffer as well as 5 μL substrate. After 4 h incubation at 37°C, caspase 3 activity was measured using a microtiter plate reader at 400 nm. The values of optical density at 400 nm were normalized to total protein content of the samples as determined by DC Protein Assay Reagents Package kit (Bio-Rad).

TUNEL Assay

DNA fission associated with apoptosis was analyzed using terminal deoxynucleotidyl transferase-mediated deoxyuridine triphosphate in situ nick end labeling (TUNEL) detection kit (Roche) following the manufacturer's instruction. The cells cultured on coverslips were rinsed with PBS, fixed with ice-cold 1% paraformaldehyde. Terminal deoxynucleotidyl transferase, a template-independent polymerase, was used to incorporate nucleotides at the sites of DNA breaks. Nuclei were stained with TO-PRO®-3. Fluorescent images were taken from three different fields on each coverslip under the confocol microscope. Apoptotic index was calculated as a percentage according to the following formula: TUNEL-positive nuclei number / the number of total cell nuclei.

Mitochondrial Membrane Potential ($\Delta\Psi_m$) Assay

Tetramethylrhodamine ethyl ester (TMRE) is a lipophilic positively charged dye and can penetrate living cells and enter the negatively charged mitochondria where it accumulates in an inner-membrane potential-dependent manner. When the $\Delta\Psi_m$ collapses in apoptotic cells, TMRE no longer accumulates inside the mitochondria and becomes more evenly distributed throughout the cytosol. When dispersed in this manner, overall cellular fluorescence levels decrease dramatically and this event can easily be visualized by fluorescence microscopy. The wavelengths of excitation (λ_{ex}) and emission (λ_{em}) for TMRE are 548 nm and 573 nm, respectively. Neurons cultured on glass coverslips were loaded with 50 nM TMRE (Invitrogen) for 20 min at room temperature. TMRE fluorescence intensity representing $\Delta\Psi_m$ was recorded under the confocol microscopy with a 60×1.4 numerical aperture oil immersion objective (Nikon). Imaging conditions such as gain levels (115) and confocal aperture size (90 μm) were held constant. Images were taken from six random fields per coverslip. Data were analyzed by ImageJ software 1.41 (Wayne Rasband).

Labeling Mitochondria

Ten days after NSCs were cultured in neuronal differentiation medium, differentiated neurons were transduced with the virus CellLight™ mitochondria-GFP (green fluorescence protein) (Invitrogen) for 24 h to label the mitochondria according to the protocol provided by the company. This fluorescent protein-based reagent contains the leader sequence of E1-alpha pyruvate dehydrogenase fused to emerald GFP. Transduced neurons expressed GFP within mitochondria. Four days later, the labeled neurons were then used for the analysis of the effect of ketamine on the cytochrome c translocation and mitochondrial fission. Transduction efficiency was calculated as the ratio between GFP-positive cells and total cells. GFP expression in the mitochondria was confirmed by the colocalization of GFP (green) and TMRE fluorescence (red) signals.

Distribution of Cytochrome C within Cytosol and Mitochondria

The distribution of cytochrome c in the neurons expressing GFP within mitochondria was analyzed with antibody against cytochrome c (abcam) using immufluorescence staining.

Analysis of Mitochondrial Fission

The labeled neurons (expressing GFP within mitochondria) treated with or without 100 μM ketamine for 24 h were imaged with the confocal microscope. Using Image J 1.41o software (Wayne Rasband; National Institutes of Health, USA), the fluorescent images were then converted to binary (black and white) images. Mitochondrial particles were analyzed for length, width, area, and perimeter. We then identified two factors of every single mitochondria of the investigated cells (43 cells per group). These two factors were used to score mitochondrial morphology to evaluate the status of mitochondrial fission and fusion as previously described:[30,31] aspect ratio (AR) and form factor (FF). AR, the ratio between the major and the minor axes of the ellipse, represents the length of the mitochondria. FF ($\text{perimeter}^2/4\pi*\text{area}$) indicates the degree of mitochondrial branching.[32] Both parameters having a minimal value of 1 represent a perfect circle. Mitochondria in healthy neurons have high values of AR and FF representing the elongated tubular mitochondria and the increase of mitochondrial complexity (length and branching), respectively. Three investigators were responsible for performing the experiments, acquiring the images, and analyzing the data independently. Two investigators were responsible for performing the experiments and acquiring the images; and the third (blinded) individual analyzed the data.

ROS Measurement

Cellular ROS were assayed using both 5-(and-6)-chloromethyl-2′, 7'-dichlorodihydrofluorescein diacetate, acetyl ester (CM-H_2DCFDA) and MitoSOX red (Invitrogen). CM-H_2DCFDA, a ROS-sensitive membrane permeable fluorescent probe, has been used extensively to measure cellular ROS (e.g, H_2O_2), but it does not measure superoxide directly. Upon penetration into the cells, the acetate groups of CM-H_2DCFDA are cleaved by cytoplasmic esterases to form membrane impermeable non-fluorescent CM-H_2DCF trapped within the cells. CM-H_2DCF is then rapidly oxidized by ROS into a fluorescent dye dichlorodihydrofluorescein (DCF). The increase of DCF fluorescence serves as a measure of ROS generation. MitoSOX red is a selective indicator of mitochondrial superoxide which is catalyzed to form many ROS members like H_2O_2 and $OH^{\cdot -}$ radicals by superoxide dismutase enzymes and also by autodismutation reactions. MitoSOX™ red is a poorly fluorescent compound carrying a charge that results in the selective accumulation of this probe within the mitochondria. After reaction with the superoxide anion, oxidized MitoSOX™ red produces DNA sensitive fluorochromes that generate a red fluorescence. (A) CM-H_2DCFDA assay. Neurons were loaded with 10 μM CM-H_2DCFDA for 30 min in the presence/absence of ketamine with or without Trolox followed by 20-min washout. The neuron-contained coverslips were placed in a polycarbonate recording chamber (Warner Instruments) on the stage of confocal microscope. DCF fluorescence ($\lambda_{ex}/\lambda_{em}$=495/520 nm) was visualized using the confocol microscope within 8 min. Imaging conditions for ROS data acquisition such as gain levels (120) and confocal aperture size (90 μm) were held constant between different groups. DCF intensity was then quantified with ImageJ software 1.41. Results were obtained from at least 30 neurons in each of three experiments per group. (B) MitoSOX™ red assay.[33,34] Neurons were treated with or without 100 μM ketamine for 24 h. Twenty-four h later, cells were labeled with 5 μM MitoSOX red in the neuronal differentiation medium for 10 min at 37°C. After cells were washed twice at room temperature, MitoSOX red fluorescence in the cells was recorded under the confocol microscope within 8 min. The excitation and emission wavelength are $\lambda_{ex}/\lambda_{em}$ = 510/580 nm for MitoSOX red. Imaging conditions for MitoSOX red data acquisition such as gain levels (100) and confocal aperture size (90 μm) were held constant. Results were obtained from at least 30 neurons in each of three experiments per group.

Statistical Analysis

Previous studies showed that ketamine significantly decreased neuronal death based on the data that were obtained from n=3.[11,15] The study had more than n=3 when multiple groups/conditions were considered. For instance, when 2 to 6 groups were considered, there were 6 to 18 samples examined. In addition, we examined the normality of residuals from the presented data by drawing a QQ-plot of residuals using SPSS software version 15. No substantial deviations from the expected straight line pattern were found in the QQ-plots. This simultaneously evaluated the assumptions of normality and variance homogeneity. Additionally, Levene's test was used to formally assess the homogeneity of variance. With reliance on these prior studies and the residual analysis, we collected data from three independent neuronal differentiations. Reported values were expressed as the means ± standard errors of the means showing normal distribution. The statistically significant differences of raw data among groups were tested by using one-way analysis of variance using SPSS software. Tukey's post hoc test was used for pairwise comparisons, and only adjusted p-values are reported. A level of $P<0.05$ was considered to be statistically significant.

Results

Differentiation of hESCs into Neurons

hESCs were induced to differentiate into neurons *in vitro* via a four-step progression as shown in Figure 1A. Cells at different differentiation stages demonstrated different morphology and expressed different cell-specific markers. hESCs grew as colonies while cultured on MEFs and stained positive for pluripotent stem cell markers Oct-4 and SSEA-4 (Fig. 1B-a to c). hESCs were then directly differentiated into neural rosettes which were radial arrangements of columnar NSCs. Rosette cells expressed neuroepithelial cell marker PAX6 (Fig. 1B-d to e). In the rosette culture, cells were heterogeneous. Rosettes were surrounded by other non-organized cells. The radially organized rosette cells were then mechanically isolated under the microscope and cultured on matrigel-coated dishes. These enriched NSCs showed triangle-like morphology and had strong proliferation potential. NSCs were confirmed by the expression of both NSC marker nestin and proliferating marker Ki67 (Fig. 1B-f to h).

Obvious neuronal differentiation could be observed in the culture 3 days after NSCs were cultured in neuronal differentiation medium. Differentiated neurons exhibited round cell shape with small projections. Cell projections extended and the extensive neuron networks were further formed in the culture over time. Two-week-old neurons expressed neuron-specific markers β-tubulin III and MAP2 (Figs. 1C-a to c). In addition, they expressed synaptic marker synapsin-1 (Fig. 1C-d) which is exclusively localized in the regions occupied by synaptic vesicles.[35] Differentiated neurons also expressed postsynaptic protein Homer 1 (a family of postsynaptic scaffolding proteins) (Fig. 1C-e).[36] There were approximately 92% of NSCs differentiating into neurons within 2 weeks of protocol initiation.

Short-Term Exposure of Ketamine Enhances Neural Stem Cell Proliferation

NSCs were treated with 100 μM ketamine for 3 and 6 h followed by Ki67 immunofluorescence staining and BrdU assays. There were more Ki67-positive cells in the 6 h-ketamine-treated culture than in the control and 3 h-ketamine culture (Figs. 2A and B) (P=0.016 vs. 6 h no-treatment control, n=3). The influence of ketamine on the proliferation of NSCs was further analyzed by BrdU assay. Ketamine (100 μM) increased NSC proliferation after 6 h of exposure (P=0.026 vs. 6 h no-treatment control, n=3) (Fig. 2C). There were no significant differences of Ki67-positive cells and BrdU incorporation between 3 and 6 h control groups. Caspase 3 activity assay showed that ketamine treatment for up to 24 h did not induce NSC apoptosis (Fig. 2D).

Ketamine Causes Ultrastructural Abnormalities in Neurons

The effect of ketamine on the ultrastructure in the neurons was analyzed using electron microscope. As shown in Figure 3, the neurons without ketamine treatment had very elongated mitochondria. Other organelles such as Golgi apparatus appeared regular. In the 24 h of 100 μM ketamine-treated culture, clear signs of the toxic effect on the cellular ultrastructure were observed and described as follows: Large oval-shaped autophagosomes having some membrane-like material within them were found in almost every cell occupying the majority of the cytosol volume. Other notable observations were the fragmented mitochondria and the disappearance of Golgi.

Ketamine Induces Neuronal Apoptosis

In order to investigate if ketamine induces the occurrences of apoptosis in neurons, we measured caspase 3 activity and examined DNA damage by TUNEL staining. When compared with no-treatment, 24 h of 100 μM ketamine exposure significantly increased

caspase 3 activity (P=0.016, n=3) (Fig. 4A). Consistent with caspase 3 activation, more TUNEL-positive cells were observed in ketamine-treated cultures (Fig. 4B). Most cells stained positive for TUNEL were located in condensed nuclei, a hallmark of apoptosis. There were 19 ± 2% apoptotic cells after treatments with ketamine. In control, some spontaneous programmed cell death resulted in 12 ± 0.4% TUNEL-positive cells (Fig. 4C).

Ketamine Induces Neuronal Apoptosis via Mitochondria Pathway

Given that ketamine may cause mitochondrial damage, we then measured $\Delta\Psi_m$ and distribution of cyochrome c in the cells. As shown in Figure 5A, treatment of differentiated neurons with 100 μM ketamine for 24 h significantly decreased $\Delta\Psi_m$ (P=0.030, n=3). To investigate the distribution of cytochrome c within the cells, the neurons were transduced with the virus CellLight™ mitochondria-GFP (green). The expression of GFP within mitochondria was confirmed by the colocalization of GFP and mitochondrial probe TMRE signals (red) (Fig. 5B). Transduction efficiency (GFP-positive cells) was 40% (Fig. 5C). The distribution of cytochrome c was examined using immunofluorescence staining. Figure 5D showed that cytochrome c (red fluorescence) was located within mitochondria in the control culture. However, in the ketamine-treated cells, cytochrome c was released from the mitochondria into cytosol.

Ketamine Induces Mitochondrial Fission

We next examined whether ketamine altered the mitochondrial morphology. Labeled neurons expressed GFP within mitochondria, indicating mitochondrial morphology. In the control culture, mitochondria shape was mostly tubular (Figs. 6A-a and c). After treatment with 100 μM ketamine for 24 h, much shorter and smaller mitochondria were prevalent in the cells (Figs. 6A-b and d). Mitochondrial shapes were further analyzed by measuring the AR and FF. Most mitochondria in the 24 h of 100 μM ketamine-treated cells had lower values of FF (P=0.016, n=3) and AR (P=0.00020, n=3) compared to the control, indicating mitochondrial fission (Figs. 6B and C).

Ketamine Increases ROS Production in Mitochondria

ROS production was determined by DCF fluorescence in the neurons with or without ketamine treatment. There was an increase of ROS production in the neurons compared with control (P=0.000059 vs. control, n=3). Trolox, a ROS scavenger, significantly attenuated ketamine-induced ROS production (P=0.000079 vs. ketamine group, n=3) (Figs. 7A and B). Next, we examined if the increased ROS was produced within mitochondria. The labeled neurons were then treated with or without 100 μM ketamine. Twenty four hours later, the cells were loaded with MitoSOX™ red. As shown in Figures 7C and D, ketamine increased superoxide production in the mitochondria (P=0.014 vs. control, n=3). Trolox significantly decreased ketamin-mediated superoxide production in mitochondria (P=0.042 vs. ketamine + Trolox group, n=3).

ROS Acts as a Mediator of Ketamine-Induced Neuronal Apoptosis

To determine if ROS production mediates the induction of neuroapoptosis, differentiated neurons were treated with 100 μM ketamine with or without Trolox for 24 h. Trolox (250 μM) significantly reversed ketamine-induced neuronal apoptosis (TUNEL-positive cells: 12 ± 0.4, 19 ± 2, and 12 ± 1% in control, ketamine, and ketamine plus Trolox groups, respectively, n=3) (Figs. 7E and F).

Discussion

In the current study, we investigated for the first time the ketamine-induced toxicity in human NSCs and neurons using an *in vitro* hESC-related neurogenesis model. We provided novel findings on several points: (1) ketamine increased human NSC proliferation; (2) ketamine caused neuronal apoptosis via a mitochondrial pathway; (3) ketamine-induced intracellular ROS and mitochondrial superoxide productions that were accompanied by the ultrastructural abnormalities such as increased mitochondrial fission; and (4) ketamine-induced neuroapoptosis could be attenuated by the ROS scavenger Trolox.

The greatest vulnerability of developing brain to anesthetics occurs at the time of rapid synaptogenesis or so called brain growth spurt period. In rodents, this critical period lasts from approximately postnatal days 0 to 10. For rhesus monkeys, this period takes place after approximately 115 days of gestation and up to postnatal day 60. In humans, it starts from the third trimester and continues 2 to 3 years after birth.[37–39] However, it is unclear if anesthetic-induced neuronal death is the direct cause of long-term neurocognitive dysfunction. Many developmental events (e.g., neurogenesis, synaptogenesis, and neuron structure remodeling) occur within this period. Multiple sequential steps are involved in neurogenesis including NSC proliferation and the differentiation of NSCs into neurons. Thus, we have considered that neuronal cell death may not be the only consequence caused by general anesthetics. Anesthetics may perturbate neural development by influencing NSC proliferation, neurogenesis, synaptogenesis, and neuronal survival.[40–42] In the present study, we applied hESCs to establish an *in vitro* controlled neurogenesis system (Fig. 1). There are two main advantages of this experimental model used for studying anesthetic-induced developmental neurotoxicity: (1) mimicking neural developmental principles to obtain unlimited human NSCs and neurons allows the dissection of the toxic effect of anesthetics on the NSCs and neurons and the underlying mechanisms, and (2) rapidly screening the effect of various anesthetics and conditions (e.g., dose and time) on neurotoxicity.

Our current results showed that ketamine exerted potentially toxic effects on both NSCs and neurons (Figs. 2 and 3). Shorter-term exposure (6 h) caused NSC proliferation. However, prolonged ketamine exposure led to a significant increase in apoptosis only in neurons but not in NSCs (Figs. 2D and 4A), suggesting that NSCs are more resistant to cell death than neurons. The ketamine-induced NSC proliferation was also observed in rats.[43] Ketamine acts through blockade of N-methyl-D-aspartate receptors (NMDAR).[11] D(−)-2-amino-5-phosphonopentanoic acid, an NMDAR antagonist like ketamine was also reported to increase NSC proliferation in both ventricular zone in neocortical slices and in primary cultures.[44] However, a recent *in vitro* study showed that ketamine decreased rat cortical NSC proliferation.[45] The varying effects of ketamine on NSC proliferation may be due to the different models used. Abnormal proliferation of NSCs could influence neurodevelopment. For instance, the total weight of the brain was found to be increased in autistic boys.[46] Ethanol, an NMDA antagonist, has long been recognized to be neurotoxic to the developing brain. Exposure to ethanol during brain development might promote neurodevelopmental defects.[47,48] In one recent study, Nash et al. used a similar *in vitro* hESC-based neurogenesis system to study ethanol-induced early developmental toxicity. They found that ethanol induced a complex mix of phenotypic changes, including an inappropriate increase in stem cell proliferation and loss of trophic astrocytes.[49] Thus, ketamine-induced alterations in NSC proliferation might contribute to an abnormal brain development.

Neuronal apoptosis is commonly recognized as a harmful effect of anesthetics.[12,25,50,51] However, how anesthetics cause neuronal apoptosis is not well understood. The central components of the programmed cell death are a group of proteolytic enzymes called

caspases which can be activated by various types of stimulation. Loss of $\Delta\Psi_m$ and release of cytochrome c from the mitochondria are key events in initiating mitochondria-involved apoptosis.[52] The released cytochrome c activates caspase 9, which consequently induces caspase 3 activation, resulting in the cleavage of several cellular proteins, finally leading to the typical alterations related to cell apoptosis such as DNA fragmentation in cell nuclei.[17,25] In this study, there was a significant increase in the caspase 3 activity as well as TUNEL-positive cells with condensed and fragmented nuclei after 24 h ketamine exposure (Fig. 4). This result was largely in agreement with several previous studies showing that only prolonged exposure could induce neuron death. For instance, treatment with 100 μM of ketamine for 48 h resulted in the loss of 45% of neurons from fetal rats after 18–19 days gestation.[12] In addition, ketamine-induced neuronal apoptosis was accompanied by the significant decrease in $\Delta\Psi_m$ and an increase in cytochrome c release from mitochondria into cytosol (Fig. 5), suggesting that ketamine might induce neuron apoptosis via mitochondrial pathway.

Mitochondria are highly dynamic and the alterations in mitochondrial shape (fusion or fission) can affect a variety of biological processes such as apoptosis and mitosis.[53] Inhibition of mitochondrial fission was shown to prevent mitochondrial cytochrome c release and apoptotic cell death.[54] Our data showed the fragmented discrete punctiform mitochondria in the ketamine-treated culture while mitochondria shape was elongated and interconnected to the network in the control cells (Fig. 6). In addition, in response to ketamine, there was a significant increase in ROS production. Superoxide within mitochondria was also high in the ketamine-treated cells, indicating the mitochondrial origin of ROS. Trolox, a ROS scavenger, prevented ketamine-induced ROS production and cell apoptosis (Fig. 7). ROS are involved in the regulation of many physiological processes. However, overproduction of ROS under various cellular stresses can cause cell death. Mitochondria are a main source of ROS, and the primary ROS is superoxide, which is converted to H_2O_2 either by spontaneous dismutation or by the enzyme superoxide dismutase. H_2O_2 can be further transformed to OH.[55] Recent studies suggested that accumulation of ROS was associated with anesthetic-induced mitochondrial damage.[17,56] Application of antioxidant 7-nitroindazole (nitric oxide synthase inhibitor) provided protection against ketamine-induced neuronal cell death.[57] In addition, ROS was implicated in the mitochondrial fission process. Inhibition of mitochondrial fission prevented high glucose-induced ROS production.[58] Thus, mitochondrial fission may mediate the ketamine-induced neuronal apoptosis by increasing ROS production. The experimental approach used here, however, does not allow for the resolution of the complete sequence of events regarding how ketamine induces neurotoxicity. Future experiments will dissect the cooperation of mitochondria fission and ROS production in the ketamine-induced neuronal apoptosis.

In conclusion, we used the *in vitro* hESC-related neurogenesis model to study ketamine-induced human neurotoxicity, demonstrating for the first time that ketamine exerts its influence on human NSC proliferation and neuronal viability via mitochondria pathway. This stem cell-related neurogenesis system might provide a simple and promising *in vitro* model for rapid screening of anesthetic-induced neurotoxicity and studying the underlying mechanisms as well as prevention strategies to avoid these toxic effects. In addition, given the toxic effect on the neurons seen in the culture treated with 100 μM ketamine for 24 hours, short-term low dose ketamine might be a safer strategy for brief procedure or other sedation in human children.

Acknowledgments

The authors thank Aniko Szabo, Ph.D. (Associate Professor, Institute for Health and Society, Division of Biostatistics, Medical College of Wisconsin) for help with the statistical analysis.

Funding: This work was supported in part by P01GM066730, R01HL034708 from the NIH, Bethesda, MD, and by FP00003109 from Advancing a Healthier Wisconsin Research and Education Initiative Fund (to Dr. Bosnjak).

References

1. Chalon J, Tang CK, Ramanathan S, Eisner M, Katz R, Turndorf H. Exposure to halothane and enflurane affects learning function of murine progeny. Anesth Analg. 1981; 60:794–7. [PubMed: 7197490]
2. Jevtovic-Todorovic V, Hartman RE, Izumi Y, Benshoff ND, Dikranian K, Zorumski CF, Olney JW, Wozniak DF. Early exposure to common anesthetic agents causes widespread neurodegeneration in the developing rat brain and persistent learning deficits. J Neurosci. 2003; 23:876–82. [PubMed: 12574416]
3. Mazoit JX, Roulleau P, Baujard C. Isoflurane-induced neuroapoptosis in the neonatal rhesus macaque brain: isoflurane or ischemia-reperfusion? Anesthesiology. 2010; 113:1245. author reply -6. [PubMed: 20966672]
4. Slikker W Jr. Zou X, Hotchkiss CE, Divine RL, Sadovova N, Twaddle NC, Doerge DR, Scallet AC, Patterson TA, Hanig JP, Paule MG, Wang C. Ketamine-induced neuronal cell death in the perinatal rhesus monkey. Toxicological sciences : an official journal of the Society of Toxicology. 2007; 98:145–58. [PubMed: 17426105]
5. Haley-Andrews S. Ketamine: the sedative of choice in a busy pediatric emergency department. J Emerg Nurs. 2006; 32:186–8. [PubMed: 16580488]
6. Young C, Jevtovic-Todorovic V, Qin YQ, Tenkova T, Wang H, Labruyere J, Olney JW. Potential of ketamine and midazolam, individually or in combination, to induce apoptotic neurodegeneration in the infant mouse brain. Br J Pharmacol. 2005; 146:189–97. [PubMed: 15997239]
7. Loepke AW, Soriano SG. An assessment of the effects of general anesthetics on developing brain structure and neurocognitive function. Anesth Analg. 2008; 106:1681–707. [PubMed: 18499597]
8. Jevtovic-Todorovic V. Pediatric anesthesia neurotoxicity: an overview of the 2011 SmartTots panel. Anesth Analg. 2011; 113:965–8. [PubMed: 22021791]
9. Boscolo A, Starr JA, Sanchez V, Lunardi N, DiGruccio MR, Ori C, Erisir A, Trimmer P, Bennett J, Jevtovic-Todorovic V. The abolishment of anesthesia-induced cognitive impairment by timely protection of mitochondria in the developing rat brain: the importance of free oxygen radicals and mitochondrial integrity. Neurobiol Dis. 2012; 45:1031–41. [PubMed: 22198380]
10. Liu F, Paule MG, Ali S, Wang C. Ketamine-induced neurotoxicity and changes in gene expression in the developing rat brain. Curr Neuropharmacol. 2011; 9:256–61. [PubMed: 21886601]
11. Wang C, Sadovova N, Hotchkiss C, Fu X, Scallet AC, Patterson TA, Hanig J, Paule MG, Slikker W Jr. Blockade of N-methyl-D-aspartate receptors by ketamine produces loss of postnatal day 3 monkey frontal cortical neurons in culture. Toxicol Sci. 2006; 91:192–201. [PubMed: 16500925]
12. Takadera T, Ishida A, Ohyashiki T. Ketamine-induced apoptosis in cultured rat cortical neurons. Toxicol Appl Pharmacol. 2006; 210:100–7. [PubMed: 16307766]
13. Vutskits L, Gascon E, Tassonyi E, Kiss JZ. Effect of ketamine on dendritic arbor development and survival of immature GABAergic neurons in vitro. Toxicol Sci. 2006; 91:540–9. [PubMed: 16581949]
14. Mellon RD, Simone AF, Rappaport BA. Use of anesthetic agents in neonates and young children. Anesth Analg. 2007; 104:509–20. [PubMed: 17312200]
15. Wang C, Sadovova N, Fu X, Schmued L, Scallet A, Hanig J, Slikker W. The role of the N-methyl-D-aspartate receptor in ketamine-induced apoptosis in rat forebrain culture. Neuroscience. 2005; 132:967–77. [PubMed: 15857702]
16. Istaphanous GK, Howard J, Nan X, Hughes EA, McCann JC, McAuliffe JJ, Danzer SC, Loepke AW. Comparison of the neuroapoptotic properties of equipotent anesthetic concentrations of

desflurane, isoflurane, or sevoflurane in neonatal mice. Anesthesiology. 2011; 114:578–87. [PubMed: 21293251]

17. Zhang Y, Dong Y, Wu X, Lu Y, Xu Z, Knapp A, Yue Y, Xu T, Xie Z. The mitochondrial pathway of anesthetic isoflurane-induced apoptosis. J Biol Chem. 2010; 285:4025–37. [PubMed: 20007710]
18. Sun LS, Li G, Dimaggio C, Byrne M, Rauh V, Brooks-Gunn J, Kakavouli A, Wood A. Anesthesia and neurodevelopment in children: time for an answer? Anesthesiology. 2008; 109:757–61. [PubMed: 18946281]
19. Shin S, Dalton S, Stice SL. Human motor neuron differentiation from human embryonic stem cells. Stem Cells Dev. 2005; 14:266–9. [PubMed: 15969621]
20. Vidarsson H, Hyllner J, Sartipy P. Differentiation of human embryonic stem cells to cardiomyocytes for in vitro and in vivo applications. Stem Cell Rev. 2010; 6:108–20. [PubMed: 20091143]
21. Bissonnette CJ, Lyass L, Bhattacharyya BJ, Belmadani A, Miller RJ, Kessler JA. The controlled generation of functional Basal forebrain cholinergic neurons from human embryonic stem cells. Stem Cells. 2011; 29:802–11. [PubMed: 21381151]
22. Laposa R. Stem cells for Drug Screening. J Cardiovasc Pharmacol. 2011; 58:240–5. [PubMed: 21499120]
23. Domino EF, Zsigmond EK, Domino LE, Domino KE, Kothary SP, Domino SE. Plasma levels of ketamine and two of its metabolites in surgical patients using a gas chromatographic mass fragmentographic assay. Anesth Analg. 1982; 61:87–92. [PubMed: 7198883]
24. McLean RF, Baker AJ, Walker SE, Mazer CD, Wong BI, Harrington EM. Ketamine concentrations during cardiopulmonary bypass. Can J Anaesth. 1996; 43:580–4. [PubMed: 8773864]
25. Braun S, Gaza N, Werdehausen R, Hermanns H, Bauer I, Durieux ME, Hollmann MW, Stevens MF. Ketamine induces apoptosis via the mitochondrial pathway in human lymphocytes and neuronal cells. Br J Anaesth. 2010; 105:347–54. [PubMed: 20659914]
26. Campbell LL, Tyson JA, Stackpole EE, Hokenson KE, Sherrill H, McKeon JE, Kim SA, Edmands SD, Suarez C, Hall AC. Assessment of general anaesthetic cytotoxicity in murine cortical neurones in dissociated culture. Toxicology. 2011; 283:1–7. [PubMed: 21277931]
27. Mak YT, Lam WP, Lu L, Wong YW, Yew DT. The toxic effect of ketamine on SH-SY5Y neuroblastoma cell line and human neuron. Microsc Res Tech. 2010; 73:195–201. [PubMed: 19725066]
28. Ibla JC, Hayashi H, Bajic D, Soriano SG. Prolonged exposure to ketamine increases brain derived neurotrophic factor levels in developing rat brains. Current drug safety. 2009; 4:11–6. [PubMed: 19149520]
29. Brambrink AM, Evers AS, Avidan MS, Farber NB, Smith DJ, Martin LD, Dissen GA, Creeley CE, Olney JW. Ketamine-induced neuroapoptosis in the fetal and neonatal rhesus macaque brain. Anesthesiology. 2012; 116:372–84. [PubMed: 22222480]
30. Merrill RA, Dagda RK, Dickey AS, Cribbs JT, Green SH, Usachev YM, Strack S. Mechanism of neuroprotective mitochondrial remodeling by PKA/AKAP1. PLoS biology. 2011; 9:e1000612. [PubMed: 21526220]
31. Cribbs JT, Strack S. Functional characterization of phosphorylation sites in dynamin-related protein 1. Methods in enzymology. 2009; 457:231–53. [PubMed: 19426871]
32. Krebiehl G, Ruckerbauer S, Burbulla LF, Kieper N, Maurer B, Waak J, Wolburg H, Gizatullina Z, Gellerich FN, Woitalla D, Riess O, Kahle PJ, Proikas-Cezanne T, Kruger R. Reduced basal autophagy and impaired mitochondrial dynamics due to loss of Parkinson's disease-associated protein DJ-1. PLoS One. 2010; 5:e9367. [PubMed: 20186336]
33. Liu Y, Schubert DR. The specificity of neuroprotection by antioxidants. J Biomed Sci. 2009; 16:98. [PubMed: 19891782]
34. Brescia F, Sarti M, Massa R, Calabrese ML, Sannino A, Scarfi MR. Reactive oxygen species formation is not enhanced by exposure to UMTS 1950 MHz radiation and co-exposure to ferrous ions in Jurkat cells. Bioelectromagnetics. 2009; 30:525–35. [PubMed: 19475646]

35. Hirokawa N, Sobue K, Kanda K, Harada A, Yorifuji H. The cytoskeletal architecture of the presynaptic terminal and molecular structure of synapsin 1. J Cell Biol. 1989; 108:111–26. [PubMed: 2536030]
36. Kammermeier PJ. Endogenous homer proteins regulate metabotropic glutamate receptor signaling in neurons. J Neurosci. 2008; 28:8560–7. [PubMed: 18716215]
37. Dobbing J, Sands J. Comparative aspects of the brain growth spurt. Early Hum Dev. 1979; 3:79–83. [PubMed: 118862]
38. Morrow BA, Roth RH, Redmond DE Jr. Sladek JR Jr. Elsworth JD. Apoptotic natural cell death in developing primate dopamine midbrain neurons occurs during a restricted period in the second trimester of gestation. Exp Neurol. 2007; 204:802–7. [PubMed: 17313945]
39. Dekaban AS. Changes in brain weights during the span of human life: relation of brain weights to body heights and body weights. Ann Neurol. 1978; 4:345–56. [PubMed: 727739]
40. Stratmann G, Sall JW, May LD, Bell JS, Magnusson KR, Rau V, Visrodia KH, Alvi RS, Ku B, Lee MT, Dai R. Isoflurane differentially affects neurogenesis and long-term neurocognitive function in 60-day-old and 7-day-old rats. Anesthesiology. 2009; 110:834–48. [PubMed: 19293705]
41. De Roo M, Klauser P, Briner A, Nikonenko I, Mendez P, Dayer A, Kiss JZ, Muller D, Vutskits L. Anesthetics rapidly promote synaptogenesis during a critical period of brain development. PLoS One. 2009; 4:e7043. [PubMed: 19756154]
42. Culley DJ, Boyd JD, Palanisamy A, Xie Z, Kojima K, Vacanti CA, Tanzi RE, Crosby G. Isoflurane decreases self-renewal capacity of rat cultured neural stem cells. Anesthesiology. 2011; 115:754–63. [PubMed: 21666433]
43. Keilhoff G, Bernstein HG, Becker A, Grecksch G, Wolf G. Increased neurogenesis in a rat ketamine model of schizophrenia. Biol Psychiatry. 2004; 56:317–22. [PubMed: 15336513]
44. Hirasawa T, Wada H, Kohsaka S, Uchino S. Inhibition of NMDA receptors induces delayed neuronal maturation and sustained proliferation of progenitor cells during neocortical development. J Neurosci Res. 2003; 74:676–87. [PubMed: 14635219]
45. Dong C, Rovnaghi CR, Anand KJ. Ketamine alters the neurogenesis of rat cortical neural stem progenitor cells. Crit Care Med. 2012; 40:2407–16. [PubMed: 22635046]
46. Courchesne E, Mouton PR, Calhoun ME, Semendeferi K, Ahrens-Barbeau C, Hallet MJ, Barnes CC, Pierce K. Neuron number and size in prefrontal cortex of children with autism. JAMA. 2011; 306:2001–10. [PubMed: 22068992]
47. Miller MW. Effects of alcohol on the generation and migration of cerebral cortical neurons. Science. 1986; 233:1308–11. [PubMed: 3749878]
48. Miller MW. Mechanisms of ethanol induced neuronal death during development: from the molecule to behavior. Alcohol Clin Exp Res. 1996; 20:128A–32A.
49. Nash R, Krishnamoorthy M, Jenkins A, Csete M. Human embryonic stem cell model of ethanol-mediated early developmental toxicity. Exp Neurol. 2011; 234:127–35. [PubMed: 22227564]
50. Zou X, Patterson TA, Sadovova N, Twaddle NC, Doerge DR, Zhang X, Fu X, Hanig JP, Paule MG, Slikker W, Wang C. Potential neurotoxicity of ketamine in the developing rat brain. Toxicological sciences : an official journal of the Society of Toxicology. 2009; 108:149–58. [PubMed: 19126600]
51. Soriano SG, Liu Q, Li J, Liu JR, Han XH, Kanter JL, Bajic D, Ibla JC. Ketamine activates cell cycle signaling and apoptosis in the neonatal rat brain. Anesthesiology. 2010; 112:1155–63. [PubMed: 20418696]
52. Budd SL, Tenneti L, Lishnak T, Lipton SA. Mitochondrial and extramitochondrial apoptotic signaling pathways in cerebrocortical neurons. Proc Natl Acad Sci U S A. 2000; 97:6161–6. [PubMed: 10811898]
53. Ong SB, Subrayan S, Lim SY, Yellon DM, Davidson SM, Hausenloy DJ. Inhibiting mitochondrial fission protects the heart against ischemia/reperfusion injury. Circulation. 2010; 121:2012–22. [PubMed: 20421521]
54. Frank S, Gaume B, Bergmann-Leitner ES, Leitner WW, Robert EG, Catez F, Smith CL, Youle RJ. The role of dynamin-related protein 1, a mediator of mitochondrial fission, in apoptosis. Dev Cell. 2001; 1:515–25. [PubMed: 11703942]

55. Brookes PS, Yoon Y, Robotham JL, Anders MW, Sheu SS. Calcium, ATP, and ROS: a mitochondrial love-hate triangle. Am J Physiol Cell Physiol. 2004; 287:C817–33. [PubMed: 15355853]

56. Wang C, Zhang X, Liu F, Paule MG, Slikker W Jr. Anesthetic-induced oxidative stress and potential protection. ScientificWorldJournal. 2010; 10:1473–82. [PubMed: 20661539]

57. Wang C, Sadovova N, Patterson TA, Zou X, Fu X, Hanig JP, Paule MG, Ali SF, Zhang X, Slikker W Jr. Protective effects of 7-nitroindazole on ketamine-induced neurotoxicity in rat forebrain culture. Neurotoxicology. 2008; 29:613–20. [PubMed: 18456338]

58. Yu T, Robotham JL, Yoon Y. Increased production of reactive oxygen species in hyperglycemic conditions requires dynamic change of mitochondrial morphology. Proc Natl Acad Sci U S A. 2006; 103:2653–8. [PubMed: 16477035]

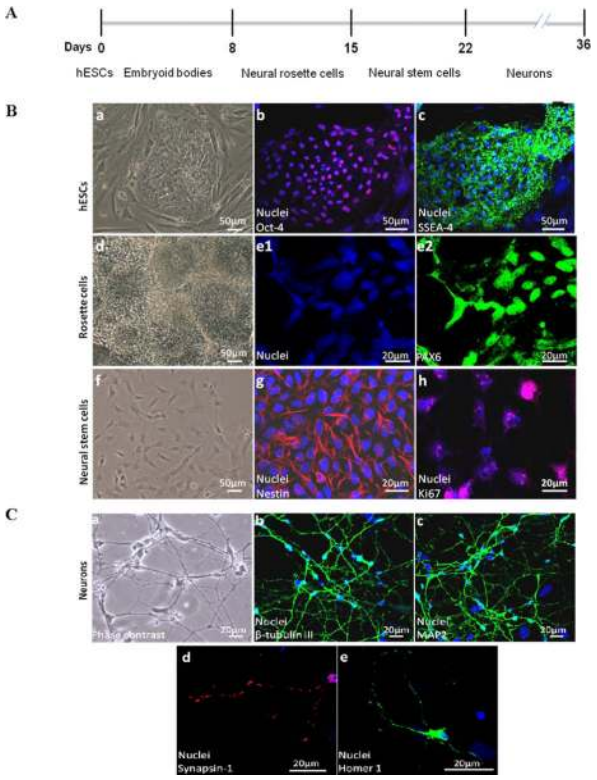

Figure 1.

Differentiation of hESCs into neurons. A, Timeline for the generation of neurons from human embryonic stem cells (hESCs). hESCs were induced to differentiate into neurons *in vitro* via a four-step program that includes embryoid body formation, neural rosette cell differentiation, neural stem cell (NSC) expansion, and neuronal differentiation. B, Differentiation of hESCs into NSCs. (a to c) Characterization of hESCs. hESCs grew as uniform flat colonies on mouse embryonic fibroblasts (MEF) (a). hESCs expressed pluripotent stem cell markers Oct-4 (b, pink) and SSEA-4 (c, green). Blue are cell nuclei. (d and e) Characterization of rosette cells. Rosette cells were observed 15 days after the initiation of neural differentiation from hESCs (d). They expressed neuroepithelial cell marker PAX6 (e2, green) in the cell nuclei (e1, blue). (f to h) Characterization of NSCs. NSCs grew as a monolayer (f). They were positive for NSC-specific marker nestin (g, red) and proliferating marker Ki67 (h, red). Blue are cell nuclei. Scale bars are 50 μm in Figures a to d, and f; 20 μm in Figures e, g, and h. C, Characterization of differentiated neurons from hESCs. Two weeks after culturing in neuronal differentiation medium, NSCs demonstrated neuron-like morphology with a small round cell body extending long projections (a). Differentiated cells were positive for neuron-specific markers β-tubulin III (b, green) and MAP2 (c, green). In addition, these differentiated neurons expressed synapse-specific marker synapsin-1 (d, red) and postsynaptic marker Homer 1 (e, green). Scale bar=20 μm.

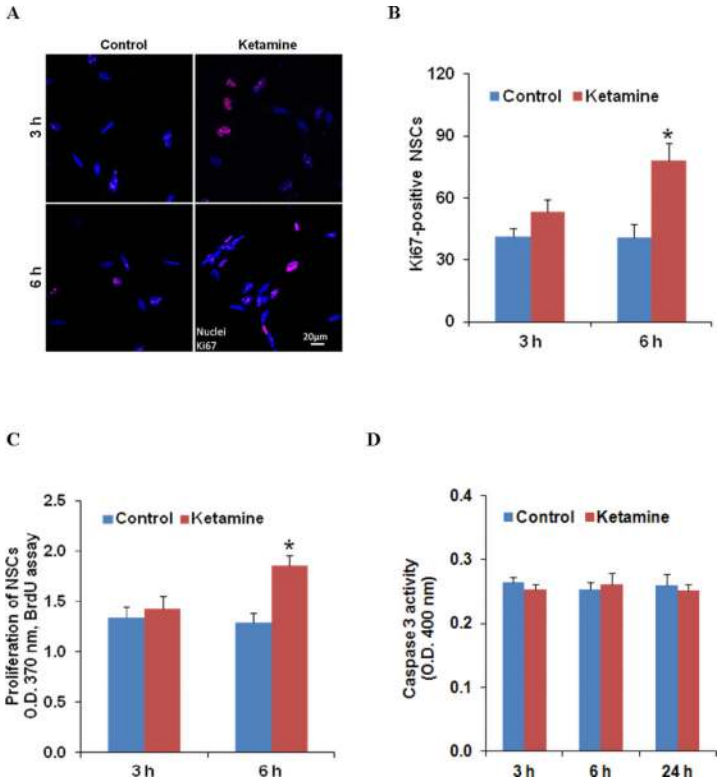

Figure 2.

Short-term exposure of 100 μM ketamine enhances NSC proliferation but does not induce NSC death. A, Ketamine increases Ki67-positive NSCs. NSCs were treated with ketamine for 3 and 6 h. The expression of Ki67 (red), a proliferating cell marker, was analyzed using immunofluorescence staining. Blue are cell nuclei. B, Ketamine significantly increases Ki67-positive NSCs (*P<0.05) vs. 6 h no-treatment control, n=3). C, Ketamine increases NSC proliferation analyzed by bromodeoxyurindine incorporation. Ketamine significantly enhanced NSC proliferation after 6 h of exposure (*P<0.05 vs. 6 h no-treatment control,n=3). D, Ketamine does not cause NSC apoptosis analyzed by caspase 3 activity (n=7). The 95% confidence intervals for the difference (adjusted by Tukey's method) were (−0.012, 0.037) for 3 h-control vs. 3 h-ketamine, (−0.032, 0.017) for 6 h-control vs. 6 h-ketamine, and (−0.016, 0.033) for 24 h-control vs. 24 h-ketamine.

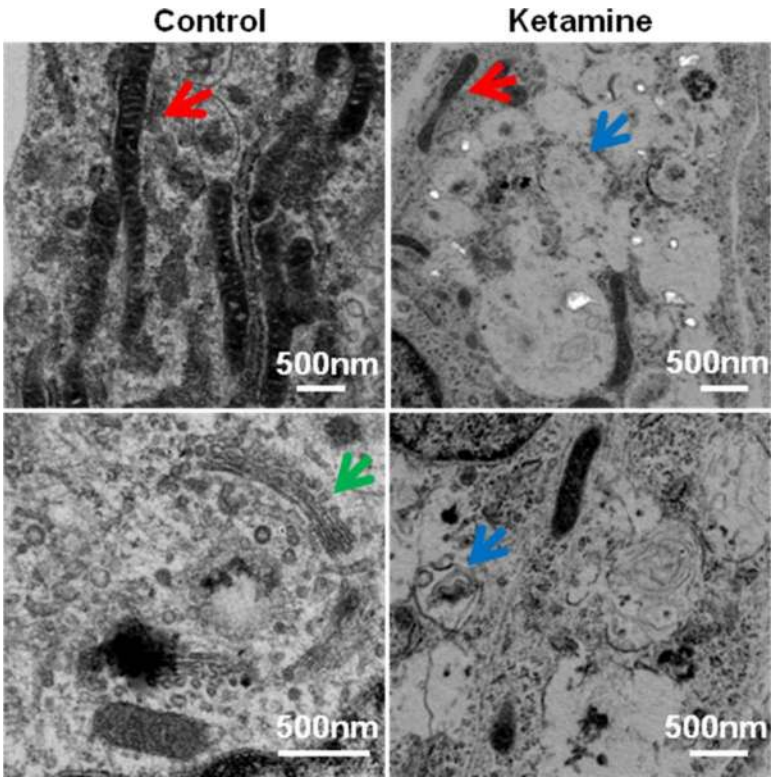

Figure 3. Ketamine causes abnormal cellular changes in ultrastructure

Representative electron microscope images of differentiated neurons treated with the indicated concentrations of ketamine for 24 h. Ketamine-treated neurons showed clear signs of the toxic effect on the cellular ultrastructure. Abnormal ultrastructure of neurons included mitochondrial fragmentation and many autophagosomes with or without being packed with dense amorphous material. In addition, Golgi structures in the 100 μM ketamine-treated cells were not observed. Red, blue, and green arrows indicate mitochondria, autophagosome, and Golgi, respectively. Scale bars=500 nm.

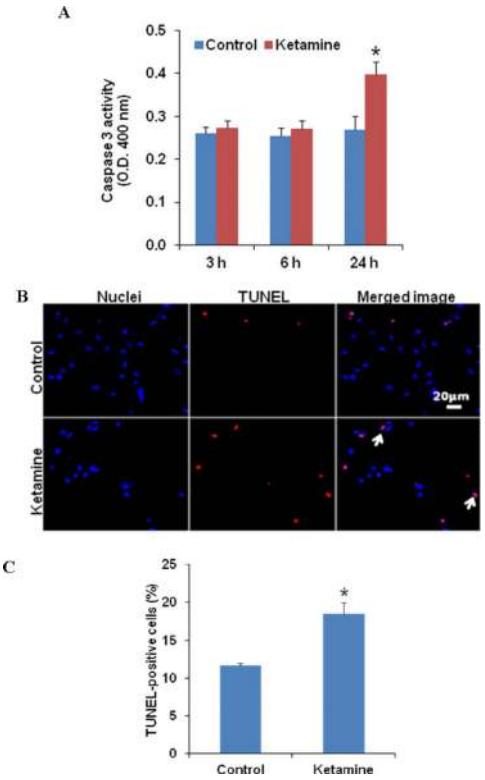

Figure 4. Ketamine increases cleaved caspase 3 activity and TUNEL-positive apoptotic cells

A, Measurement of caspase 3 activity in the lysate of neurons treated with or without 100 μM ketamine for 24 h. B, TUNEL staining used to identify DNA damage in cells after a 24-h exposure to 100 μM ketamine. TO-PRO®-3 was used to stain DNA (blue). Overlaid images demonstrate that most TUNEL signals were located in the condensed or fragmented nuclei in ketamine-treated cells. The representative fragmented nuclei are indicated using arrows. Scale bars are 20 μm. C, Quantification of the percentage of TUNEL-positive cells. Significant increases in caspase 3 activity and TUNEL-positive cells were observed in ketamine-treated culture compared with untreated controls (*P<0.05 vs. control, n=3).

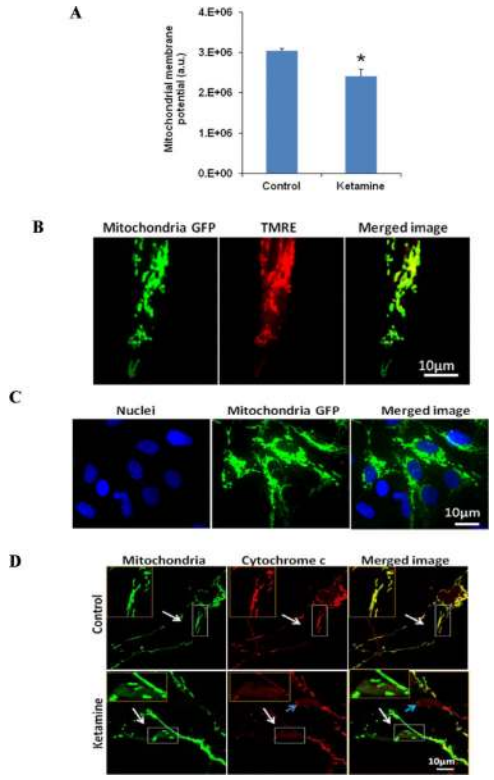

Figure 5. Ketamine decreases mitochondrial membrane potential ($\Delta\Psi_m$) and increases cytochrome c release form mitochondria into cytosol

A, $\Delta\Psi_m$ assay. Cells were loaded with mitochondrial probe TMRE and imaged with the confocol microscope. The fluorescent intensity of TMRE represents $\Delta\Psi_m$. The results show that 100 μM ketamine treatment for 24 h decreased $\Delta\Psi_m$ (*P<0.05 vs. control, n=3). B, Colocalization of TMRE and mitochondria-targeted green fluorescence protein (GFP). Differentiated neurons labeled with CellLight™ mitochondria-GFP reagent expressed GFP. The GFP-positive cells were then loaded with TMRE. Overlaid image indicates the colocalization of TMRE and mitochondria-GFP fluorescent signals, suggesting GFP expression within mitochondria. C, Representative fluorescent images of the neurons transduced with CellLight™ mitochondria-GFP reagent. Blue are cell nuclei. Transduction efficiency was 40%. D, The distribution of cytochrome c in cells. Neurons labeled with CellLight™ mitochondria-GFP reagent expressed GFP in mitochondria. The distribution of cytotochrome c in cells was analyzed by immunufluorescence staining. Column 1 is the image of mitochondria (green); column 2 is the image of cytochrome c (red); column 3 is the merged image. The inset in the top corner of each image is the magnified box indicated by white arrows. The orange color in the merged images indicates the existence of cytochrome c inside the mitochondria and the red signals in the merged images indicate the existence of cytochrome c outside the mitochondria. Ketamine treatment (100 μM, 24 h) increased cytochrome c release from mitochondria into cytosol. The concentrated cytochrome c (red signals pointed by blue arrows) outside the mitochondria that does not overlap with GFP florescence is from nontransduced cells. Scale bar=10 μm.

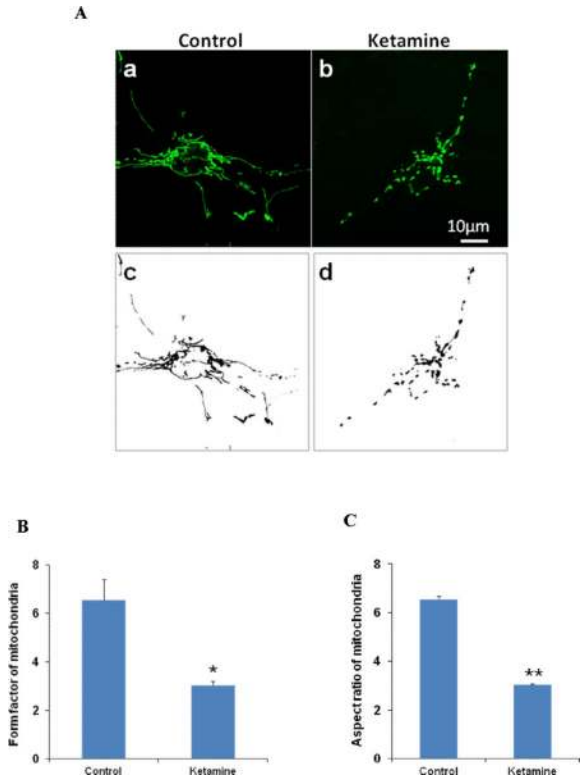

Figure 6. Ketamine increases mitochondrial fission

A, Mitochondrial shape in the cells treated with or without 100 μM ketamine for 24 h. Differentiated neurons labeled with CellLight™ mitochondria-green fluorescence protein (GFP)reagent expressed GFP in the mitochondria. Mitochondria are elongated and interconnected in the control cells (a) while mitochondria are short and disconnected in the ketamine-treated culture (b). Figure A-c and d are the black and white images of Figure A-a and b, respectively. Scale bar=10 μm. B–C, Analysis of mitochondria shapes using Image J 1.41o software. The mitochondria in the ketamine-treated neurons had significantly lower values of both form factor and aspect ratio, suggesting that ketamine increases mitochondrial fission (*P<0.05 and **P<0.01 vs. control group).

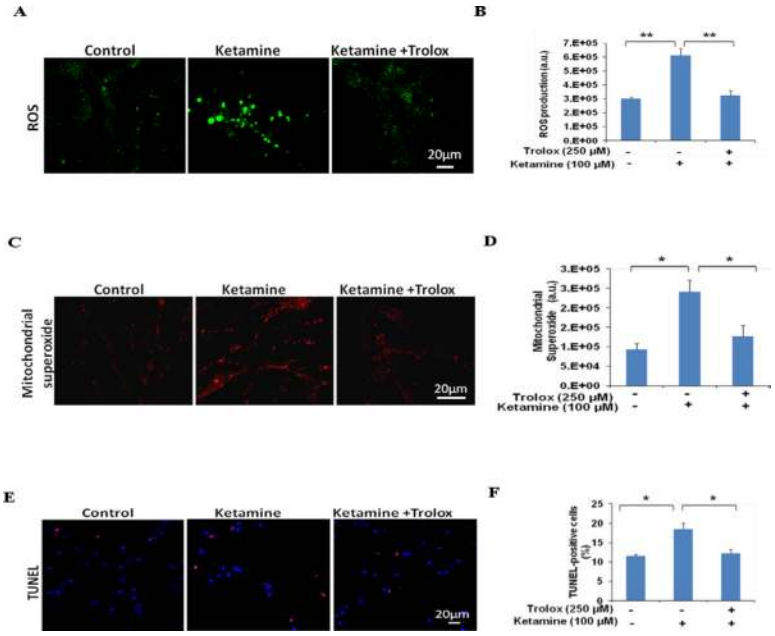

Figure 7. ROS generated from mitochondria mediates ketamine-induced neurotoxicity

Neurons were treated with 100 μM ketamine in the presence or absence of Trolox (250 μM) for 24 h and then subjected to intracellular reactive oxygen species (ROS) measurement (A and B), mitochondrial ROS assay (C and D), and TUNEL staining (E and F). A, Fluorescence images of intracellular ROS production loaded with ROS probe CM-H_2DCFDA. Green fluorescence representing intracellular ROS was recorded using the confocol microscope. B, Ketamine increases ROS production and Trolox, a ROS scavenger, attenuates ketamine-induced ROS production. **P<0.01 vs. control or ketamine + Trolox group, n=3. C, Fluorescence images of mitochondrial ROS in the culture loaded with MitoSOX™ Red. Red fluorescence indicates superoxide generation within the mitochondria. D, Ketamine induces the formation of mitochondrial superoxide and Trolox decreases mitochondrial ROS production caused by ketamine. *P<0.05 vs. control or ketamine + Trolox group, respectively. n=3. E, Fluorescence images of the cells following TUNEL staining. Blue are cell nuclei and red are the nuclei in the apoptotic cells. F, Trolox attenuates the increase of TUNEL-positive cells caused by ketamine treatment. *P<0.05 vs. control or ketamine + Trolox group, n=3.